American Journal of Pathology, Vol. 162, No. 5, May 2003

Genetic Cooperation between the Werner Syndrome Protein and Poly(ADP-Ribose) Polymerase-1 in Preventing Chromatid Breaks, Complex Chromosomal Rearrangements, and Cancer in Mice

Michel Lebel,* Josée Lavoie,† Isabelle Gaudreault,* Marc Bronsard,† and Régen Drouin†

From the Centre de Recherche en Cancérologie de l'Université Laval, Hôpital Hôtel-Dieu de Québec, Centre Hospitalier Universitaire de Quebéc (CHUQ), Québec; and Unité de Recherche en Génétique Humaine et Moléculaire,† Hôpital Saint-François d'Assise, Centre Hospitalier Universitaire de Quebéc (CHUQ), Québec, Canada*

Werner syndrome is a rare disorder characterized by the premature onset of a number of age-related diseases. The gene responsible for Werner syndrome encodes a DNA helicase/exonuclease protein. Participation in a replication complex is among the several functions postulated for the WRN protein. The poly(ADP-ribose) polymerase-1 (PARP-1) enzyme, which is known to bind to DNA strand breaks, is also associated with the DNA replication complex. To determine whether Wrn and PARP-1 enzymes act in concert during cell growth, mice with a mutation in the helicase domain of the *Wrn* gene (*Wrn*$^{\Delta hel/\Delta hel}$ mice) were crossed to *PARP-1*-null mice. Both *Wrn*$^{\Delta hel/\Delta hel}$ and *PARP-1*-null/*Wrn*$^{\Delta hel/\Delta hel}$ cohorts developed more neoplasms than wild-type animals. The tumor spectrum was the same between *PARP-1*-null/*Wrn*$^{\Delta hel/\Delta hel}$ mice and *Wrn* mutants. However, *PARP-1*-null/*Wrn*$^{\Delta hel/\Delta hel}$ mice developed neoplasms at a younger age. Mouse embryonic fibroblasts derived from such *PARP-1*-null/*Wrn*$^{\Delta hel/\Delta hel}$ mice stop dividing abruptly unlike *Wrn*$^{\Delta hel/\Delta hel}$ or *PARP-1*-null cells. *PARP-1*-null/*Wrn*$^{\Delta hel/\Delta hel}$ fibroblasts were distinguished by an increased frequency of chromatid breaks, complex chromosomal rearrangements, and fragmentation. Finally, experiments have indicated that the PARP-1 enzyme co-immunoprecipitates with the WRN protein in human 293 embryonic kidney cells. These results suggest that Wrn and PARP-1 enzymes may be part of a complex involved in the processing of DNA breaks. *(Am J Pathol 2003, 162:1559–1569)*

Werner syndrome (WS) is a rare disorder characterized by the premature onset of a number of processes associated with aging including malignancies.[1] The gene responsible for WS (*WRN*) was identified by positional cloning and the gene product contains a domain homologous to the RecQ-type DNA helicases.[2] The protein also possesses a 3′ to 5′ exonuclease activity in addition to its 3′ to 5′ helicase activity.[3–5] The WRN protein is considered a suppressor of illegitimate recombination as skin fibroblasts and lymphoblastoid cell lines made from circulating lymphocytes of WS patients exhibit variegated chromosomal translocations and deletions.[6–8] In addition, several reports have also indicated that human WS cells have abnormal telomere dynamics *in vitro* that is likely to affect replicative senescence.[9,10]

Human WS cells and murine cells with a mutation in the *WRN* gene homologue are known to be sensitive to drugs that damage DNA at replication forks such as topoisomerase inhibitors.[11] These results point to a specific activity of this protein during DNA replication. In this respect, it is interesting to note that in WS fibroblasts the S phase and the whole cell cycle are prolonged.[12] It has also been shown that the replication defect detected in WS lymphoblastoid cell lines is associated with an impaired S phase transit.[13] At the molecular level the rate of initiation of DNA replication is retarded in WS cells compared to control cells.[14,15] Finally, we have observed that the mouse Wrn protein co-purifies with the multiprotein DNA replication complex.[11,16] In addition, the WRN protein physically interacts with major components of the DNA replication fork such as proliferation cellular nuclear antigen, replication protein A, topoisomerase I, the p50 small subunit of DNA polymerase δ,[17] and flap endonuclease 1 (Fen1).[18]

The enzyme poly(ADP-ribose) polymerase-1 (PARP-1) is another component of the DNA replication complex.[19] PARP-1 physically associates with the DNA polymerase

Supported in part by grants from the Canadian Institutes of Health Research (to M. L.) and the National Cancer Institute of Canada (with funds from the Canadian Cancer Society to R. D.).

M. L. is a scholar of the Canadian Institutes of Health Research and R. D. is a senior scholar of the Fonds de la Recherche en Santé du Québec.

Accepted for publication February 5, 2003.

Address reprint requests to Michel Lebel, Ph.D.,Centre de Recherche en Cancérologie, Hôpital Hôtel-Dieu de Québec, Centre Hospitalier Universitaire de Quebéc (CHUQ), 9 McMahon St., Québec, Québec G1R 2J6, Canada. E-mail: michel.lebel@crhdq.ulaval.ca.

α-primase complex and is believed to bind to breaks on DNA damage during replication fork progression.[20] It rapidly binds to single- or double-strand breaks through its N-terminal DNA-binding domain and uses NAD (β-nicotinamide adenine dinucleotide) to synthesize poly-(ADP-ribose) on a variety of proteins including p53, topoisomerases, histones, and PARP-1 itself.[21,22] In addition, PARP-1 targets and regulates via poly(ADP-ribose) the functions of proteins involved in DNA damage checkpoints or DNA repair such as p53, DNA ligase III, DNA-PK, KU70, and XRCC1.[21,23,24] Interestingly, p53, DNA-PK and the KU70/80 complex interact with WRN protein as well.[17] Chemical or genetic abrogation of PARP-1 activity in cells leads to an increase in the frequency of sister chromatid exchanges and genomic instability[25] especially after genotoxic stresses.[22]

A number of PARP-1 knockout mice have been created by several groups.[22] Although, mice lacking a functional PARP-1 develop normally and are not cancer prone, they are hypersensitive to DNA damage.[26,27] For example, *PARP-1* knockout mice are highly susceptible to nitrosamine carcinogenicity compared to wild-type animals.[28] In addition, inhibition of PARP-1 will accelerate tumorigenesis in p53-deficient mice demonstrating a role for PARP-1 in tumor development.[29,30] Fibroblasts established from *PARP-1* mutant mice have indicated that cells acquire a slower growth rate in culture compared to wild-type fibroblasts.[31,32] In addition to a loss of proliferative capacity, *PARP-1*-null fibroblasts display increased telomere shortening compared to wild-type cells.[33] An additional report has indicated that an increase in telomere shortening is only observed in late passage cells and not in primary embryonic tissue cultures.[34] Although PARP-1 is cleaved very rapidly during apoptosis, *PARP-1*-null cells are not more prone to spontaneous apoptosis *in vitro*.[32] It is believed that it is the increased genomic instability (DNA amplification and/or loss of chromatin) that contributes to the delay in cell proliferation in *PARP-1* mutant cells.[32,34] Finally, microarray analysis on *PARP-1*-null fibroblasts have indicated that loss of PARP-1 results in deregulation of genes that encode proteins implicated in cancer initiation or progression and in normal or premature aging.[35]

Because both WRN and PARP-1 proteins are found in the DNA replication complex, it is reasonable to ask whether they act in concert in some aspect of DNA metabolism. In this study, we show that human WRN and PARP-1 enzymes can be co-immunoprecipitated *in vivo*. The roles of a potential murine Wrn/PARP-1 complex in genomic stability were further investigated in mice. Mice with a deletion of part of the helicase domain of the *Wrn* gene[11] were thus crossed to *PARP-1*-null mice[31] to study the phenotype of double-homozygous mice at the physiological, cellular, and chromosomal levels.

Materials and Methods

Mice and Cell Culture

Mice lacking part of the helicase domain of the *Wrn* gene and *PARP-1*-null mice were generated by homologous recombination as previously described.[11,31] Mice of all possible genotypes were generated by mating homozygous $Wrn^{\Delta hel/\Delta hel}$ individuals with *PARP-1*-null mice and intercrossing the F1 and F2 generations to obtain all four desired genotypes. Homozygous animals of each genotype were then crossed to obtain the numbers of mice indicated in the figure legends. The genetic background of all of the animals were both 129/Sv and Black Swiss (129/Sv/Black Swiss genetic background). Mice were maintained under pathogen-free conditions and fed *ad libitum* with Teklad Global (Madison, WI) 18% protein rodent diet (5% fat). Animals (from littermates) were checked three times a week for any external mass, infection, bleeding, gasping, and overall decrease or change in activity or behavior. Animals that became immobile or moribund were then sacrificed for histological examination of their organs as described previously.[36] Mice with skin lesions were sacrificed as soon as there was a sign of infection in the lesion.

Generation and maintenance of the embryonic fibroblasts has been described previously.[37] Briefly, cells were maintained in low-glucose Dulbecco's modified Eagle's medium supplemented with 10% heat-inactivated calf serum at 37°C in an atmosphere of 5% CO_2. Cell proliferation was determined by plating 5×10^4 cells in six-well plates. The cultures were maintained for up to 11 days with changing media every other day. Cells were counted with trypan blue on a hemocytometer. Data were plotted on a graph and cell growth was calculated from the slope of each curve (portion of the curve representing the logarithmic phase of the culture). Human 293 embryonic kidney cells were maintained in Dulbecco's modified Eagle's medium supplemented with 10% fetal bovine serum.

Protein Analysis

Protein extraction, immunoprecipitations, and Western blotting analyses were performed as described.[16] Polyclonal antibodies against the C-terminus and the N-terminus portion of human WRN were purchased from Santa Cruz Biotechnology (Santa Cruz, CA) and Novus Biologicals (Littleton, CO), respectively. The monoclonal antibody against the N-terminus portion of human PARP-1 was purchased from Transduction Laboratories (Lexington, KY). The polyclonal antibody against the C-terminus portion of human PARP-1 was purchased from Santa Cruz Biotechnology. Finally, all horseradish peroxidase-conjugated secondary antibodies were purchased from Amersham. Proteins on the Western blots were visualized using an ECL kit (Amersham). All antibodies were used as indicated by the manufacturers.

Chromosome Analysis

For each genotype, primary mouse embryonic fibroblasts (MEFs at the indicated population doublings) derived from three embryos of at least two litters were cultured for chromosome analysis. Cells were arrested by adding colcemid to a final concentration of 40 ng/ml for 1 to 3

hours. Cells were then harvested, treated with a hypotonic solution (75 mmol/L KCl) at pH 8.0 for 30 minutes at 37°C, and fixed three times in cold Carnoy's fixative (3 vol of methanol/1 vol of acetic acid) for 15 minutes.[38] Cells were resuspended in fresh fixative and dropped onto glass slides in a 40% humidity chamber at 28°C (Thermotron Industries, Holland, MI). The slides were placed overnight on a warm plate at 60°C before performing chromosome banding. G-band patterns were generated using the GTW (G-bands using trypsin and Wright staining) banding technique. The banding was produced by treating the slides in 0.2× Enzar-T trypsin (Intergen) for 1 to 2 minutes, followed by one wash in pure ethanol, and finally by a 3-minute staining in 8% Wright solution. Chromosomes of 200 metaphases were counted for all four genotypes. To study chromosomal rearrangements, 100 metaphases were analyzed and 15 metaphases karyotyped for the wild-type MEFs.[39] For the other genotypes, 150 metaphases were analyzed and 30 karyotyped. The results coming from the different embryos were pooled.

Primed in Situ *Labeling*

Primed *in situ* labeling was used to determine telomere length on chromosomes harvested from MEFs derived from two embryos per genotype at 10 to 12 population doublings.[40–42] The slides were denatured in 10 mmol/L NaOH/1 mol/L NaCl for 30 seconds at room temperature and then dehydrated in ethanol (70%, 80%, and 100%) at 4°C. Primed *in situ* labeling reaction solution that contained 4 μl of each of 2.5 μmol/L dATP, dCTP, and 0.25 μmol/L dTTP, 1 μl of 1 mmol/L digoxigenin-11-dUTP (Roche Molecular Biochemicals), 4 μl of 7.5 μmol/L primer $[(CCCTAA)_7]$, 2.5 U *Taq* polymerase (Roche Molecular Biochemicals), 5 μl of 10× PCR buffer and distilled water for a total volume of 50 μl was added on the denatured slides, which were then covered with a coverslip. A single-step primer annealing and strand elongation was performed at 62.5°C for 10 minutes on a thermocycler (PTC-100 16MS slide bloc; MJ Research). At the end of the reaction, the slides were transferred into phosphate-buffered saline (PBS) at 62.5°C for 1 minute and in washing buffer (4× standard saline citrate, 0.2% Tween 20) at room temperature for 5 minutes. To visualize the digoxigenin-labeled DNA *in situ*, 50 μl of 1% anti-digoxigenin-rhodamine (Roche Molecular Biochemicals) was applied and the slides were covered with a coverslip. After incubation in a moist chamber at 37°C for 30 minutes, the slides were washed in washing buffer (4× standard saline citrate, 0.2% Tween 20) at room temperature for 5 minutes and then in PBS at room temperature for 5 minutes. Chromosome spreads were counterstained using 125 ng/ml of 4′,6-diamino-2-phenylindole mixed with 1 mg/ml of ρ-phenylenediamine (Sigma).

Image Analysis and Telomere Measurement Analysis

All slides were examined under a Leica DMRB fluorescence microscope equipped with a JAI M300 charge-coupled device camera with a Synchro4 interface board coupled to the Metasystems *in situ* imaging system (ISIS) software version 4.1.12 and quantified by digital image analysis using the telomere measurement software. Integration times were typically 0.04 second for the 4′,6-diamino-2-phenylindole counter stain and 0.6 second for the rhodamine telomere signal. Optimization of the labeling reaction resulted in a mean telomere detection efficiency of ~98%. A good correlation between the values derived from sister chromatid telomere pairs was observed (data not shown). This observation suggests that the measured telomere fluorescence intensity values are directly related to telomere length.[43]

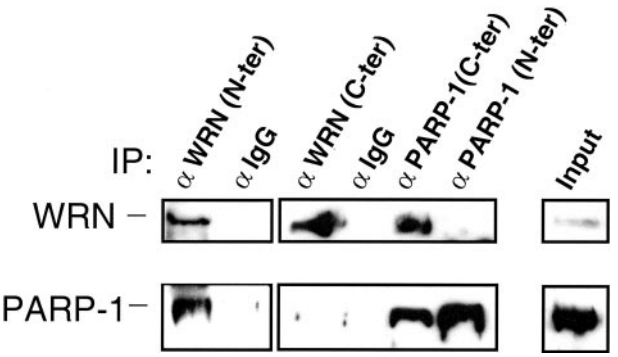

Figure 1. Co-immunoprecipitation of human WRN protein with the PARP-1 enzyme. Approximately 2 mg of protein from human 293 embryonic kidney cells were immunoprecipitated with antibodies against the N-terminus or the C-terminus region of human WRN protein and antibodies against the C-terminus or the N-terminus region of human PARP-1. Control antibodies were of the same IgG species. The immunoprecipitates were analyzed by Western blotting with the anti-WRN antibody (WRN, **top**) and an antibody against the human PARP-1 enzyme (PARP-1, **bottom**). Proteins were revealed with an ECL kit. The αWRN (N-ter) antibody is from Novus Biologicals. The αPARP-1 (N-ter) antibody is from Transduction Laboratories. The αWRN (C-ter) and αPARP-1 antibodies are from Santa Cruz Biotechnology. The **input lane** corresponds to 20 μg of total cell lysate that was analyzed on a different gel.

Results

Co-Immunoprecipitation of the WRN Protein with the PARP-1 Enzyme

Cellular fractionation experiments have indicated that both the murine Wrn and PARP-1 proteins co-purify with the multiprotein DNA replication complex.[16,19] To determine whether PARP-1 directly interacts with the WRN enzyme, immunoprecipitation experiments were performed with several different antibodies against WRN or PARP-1 on human 293 embryonic kidney cells. Human cells were used in these experiments because our antibodies against the murine Wrn enzyme did not immunoprecipitate the mouse Wrn protein. A polyclonal antibody against the N-terminus region of the human WRN protein co-immunoprecipitated the PARP-1 enzyme as revealed by Western blotting (Figure 1). In contrast, antibodies against the C-terminus portion of human WRN did not immunoprecipitate the PARP-1 enzyme. In similar sets of experiments, the PARP-1 enzyme was immunoprecipitated with antibodies against either the N-terminus or the C-terminus portions of the enzyme. As shown in Figure 1,

Table 1. Proportion (%) of *Parp-1*$^{-/-}$/*Wrn*$^{\Delta hel/\Delta hel}$, *Wrn*$^{\Delta hel/\Delta hel}$, *Parp-1*$^{-/-}$ and Wild-Type Mice that Showed Symptoms

Symptoms*	Wild type (n = 33)	*Wrn*$^{\Delta hel/\Delta hel}$ (n = 55)	*Parp-1*$^{-/-}$ (n = 18)	*Parp-1*$^{-/-}$/*Wrn*$^{\Delta hel/\Delta hel}$ (n = 38)†
Animals with hyperplasia or neoplasia	21	46‡	–§	47‡
Animals with multiple types of neoplasias	27	9‡	11	18‡¶
Unknown cause of death	12	20	–	15
Myocardial fibrosis	9	59‡	6	37‡
Myeloid hyperplasia	3	9‡	6	8‡
Inflammation (eye, lung, gut, or bladder)	15	17	22	18
Polycystic endometrium	9	4	6	13
Myeloid leukemia	12	6	–	8
Hepatocellular carcinoma	–	2	6	8
Ovarian neoplasias	3	4	–	3
Pancreatic neoplasias	3	2	–	3
Inflammation of uterus	–	9	–	8
Hepatoma	–	9	–	3
Mammary carcinoma	–	4	–	8
Thymic lymphoma	–	6	–	5
Lung adenocarcinoma	–	2	–	8
Rectal prolapsis	–	6	–	3
Harderian hyperplasia or dysplasia	–	4	–	5
Skin papilloma	3	–	–	5
Gastro-intestinal occlusion	–	–	–	5
Hemangioma	–	–	–	3
Bronchial adenoma	–	2	–	–
Hyperplasia of the prostate	–	2	–	–
Granulocyte sarcoma	–	2	–	–
Gastric or intestinal polyps	–	2	–	–

*List of phenotypes observed in mice aged between 1 and 24 months of age.
†n, The number of mice analyzed.
‡Chi-square-test compared to wild-type animals significant, $P < 0.05$.
§–, No symptom.
¶Chi-square test compared to *Wrn*$^{\Delta hel/\Delta hel}$ mice significant, $P < 0.05$.

both types of antibody immunoprecipitated PARP-1. However, stripping and reprobing of the blots with an antibody against the WRN protein revealed that WRN is detected in the immunoprecipitate only when the antibody against the C-terminus portion of PARP-1 is used (Figure 1). These experiments suggest a WRN/PARP-1 complex present in human 293 embryonic kidney cells.

A Deficiency of PARP-1 Protein in Wrn Mutant Mice Accelerates the Pathologies

To assess the joint role of PARP-1 and Wrn in specific mouse pathology including neoplasm progression, *PARP-1*-null and *Wrn*$^{\Delta hel/\Delta hel}$ mice were crossed to generate *PARP-1*-null/*Wrn*$^{\Delta hel/\Delta hel}$ animals. Littermates of all genotypes were then carefully followed throughout 2 years and scored for the occurrence of neoplasms or any signs of pathology. The average litter size for wild-type animals was 8.5 pups per litter (18 litters) and 6.9 pups per litter (17 litters) for the *Wrn*$^{\Delta hel/\Delta hel}$ mice. In contrast, the average litter size for the *PARP-1*-null mice was 4.8 pups per litter (26 litters) as described previously.[22] Finally, the average litter size for *PARP-1*-null/*Wrn*$^{\Delta hel/\Delta hel}$ animals was 4.1 pups per litter (28 litters) which is not significantly different from *PARP-1*-null mice. This indicates that *PARP-1*-null/*Wrn*$^{\Delta hel/\Delta hel}$ survived embryogenesis. There was no significant difference in average body weight between mice of all four genotypes. As indicated in Table 1, *Wrn*$^{\Delta hel/\Delta hel}$ mutant mice were remarkable with respect to the variety of illnesses and neoplasms they developed[36] compared to wild-type animals. As described before,[31,32] *PARP-1*-null mice developed few pathological phenotypes. These mice developed alopecia of the skin, epidermal hyperplasia, or infections. *PARP-1*-null animals with large skin lesions had to be sacrificed as such lesions became infected and were considered life threatening by the veterinarian. Skin lesions were detected in ~17% of the *PARP-1*-null mice. Such a phenotype was not detected in wild-type or *Wrn*$^{\Delta hel/\Delta hel}$ mutant mice. Approximately 10% of the *PARP-1*-null/*Wrn*$^{\Delta hel/\Delta hel}$ mice developed skin lesions similar to *PARP-1*-null mice. Finally, Table 1 indicates that *PARP-1*-null/*Wrn*$^{\Delta hel/\Delta hel}$ mice could potentially develop any of the pathologies observed with wild-type, *Wrn*$^{\Delta hel/\Delta hel}$, or *PARP-1*-null mice.

The age of each dissected animal was plotted on a graph for statistical analysis (Figure 2A). At first glance, Figure 2A indicates that *PARP-1*-null/*Wrn*$^{\Delta hel/\Delta hel}$ mice developed some types of pathology sooner than *Wrn*$^{\Delta hel/\Delta hel}$ mutant or wild-type animals. Log-rank tests on Figure 2A indicate that the difference between disease-free *PARP-1*-null/*Wrn*$^{\Delta hel/\Delta hel}$ and *Wrn*$^{\Delta hel/\Delta hel}$ mutant mice with time is significant ($P < 0.0008$). The difference between *Wrn*$^{\Delta hel/\Delta hel}$ mutant mice and wild-type mice is also significant ($P < 0.0001$).

Statistical analyses were also performed on the percentage of sick mice at three different ranges of ages (Figure 2B). Between 6 and 12 months of age, 21% of *PARP-1*-null/*Wrn*$^{\Delta hel/\Delta hel}$ and 17% of *PARP-1*-null mice were sick. All wild-type animals and 93% of *Wrn*$^{\Delta hel/\Delta hel}$

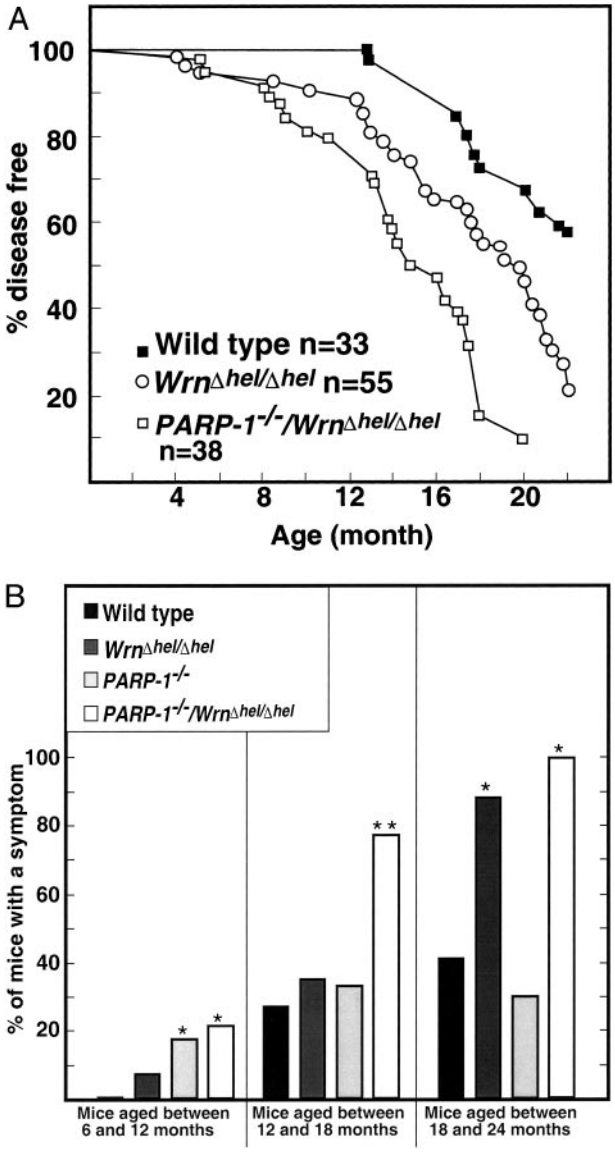

Figure 2. A: Percentage of disease-free animals from mice throughout a period of 22 months. Animals were sacrificed for pathological examination when they became moribund. The numbers of animals (n) in this survey are indicated for each genotype. **B:** Percentage of mice with a symptom at a different range of ages. The numbers of animals for each genotype are the same as Table 1. *, Indicates a significant difference (t-test, $P < 0.05$) compared to wild-type mice; **, indicates a significant difference (t-test, $P < 0.05$) compared to both wild-type and $Wrn^{\Delta hel/\Delta hel}$ mice.

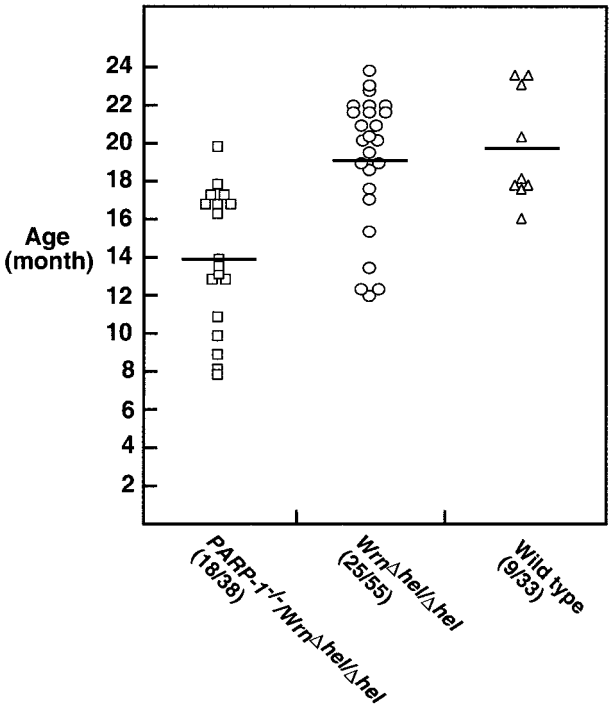

Figure 3. Age of animals with benign and/or malignant neoplasms. Wild-type, $Wrn^{\Delta hel/\Delta hel}$, and *PARP-1*-null/$Wrn^{\Delta hel/\Delta hel}$ mutant mice with neoplasms are plotted on this graph. Each **symbol** in the graph represents one sick animal. The **horizontal bars** represent the mean age for each genotype. The number of animals with neoplasms are indicated for each genotype.

mutant mice were healthy. The difference between *PARP-1*-null/$Wrn^{\Delta hel/\Delta hel}$ or *PARP-1*-null mice and wild-type animals is significant (t test; $P < 0.05$). Between 12 and 18 months of age, 77% of *PARP-1*-null/$Wrn^{\Delta hel/\Delta hel}$ were sick. In contrast, 27% to 35% of wild-type, $Wrn^{\Delta hel/\Delta hel}$ mutant, and *PARP-1*-null mice were sick. The differences between *PARP-1*-null/$Wrn^{\Delta hel/\Delta hel}$ mice and animals form all of the other genotypes were significant (t-test; $P < 0.05$). Finally, all *PARP-1*-null/$Wrn^{\Delta hel/\Delta hel}$ mice and 88% of $Wrn^{\Delta hel/\Delta hel}$ mutant animals were sick by 24 months. In contrast, less than 42% of wild-type or *PARP-1*-null animals were sick. These results indicate that *PARP-1*-null/$Wrn^{\Delta hel/\Delta hel}$ mice develop several pathological symptoms sooner than animals of the other genotypes analyzed in this study. However, it takes at least 12 months to see a significant difference between *PARP-1*-null/$Wrn^{\Delta hel/\Delta hel}$ and $Wrn^{\Delta hel/\Delta hel}$ mice.

Mutant Mice Develop Multiple Types of Neoplasms

As indicated above, *PARP-1*-null/$Wrn^{\Delta hel/\Delta hel}$ mice appeared sick at an earlier age than wild-type or $Wrn^{\Delta hel/\Delta hel}$ animals. This was so even though all animals were housed under the same conditions. Some of these animals showed a complex phenotype including infections or cardiac fibrosis in addition to neoplasms. In several instances, it was impossible to determine whether the observed cardiac fibrosis or infections were incidental to metabolic system or immune system disorders. As both Wrn and PARP-1 enzymes are involved in genomic stability, an important feature deregulated in cancer, we concentrated our next analyses on animals that were diagnosed with neoplasms. As shown in Table 1, 27% of wild-type animals (9 of 33 mice) developed some type of hyperplasia or neoplasia at the age of 13 to 24 months. The most common proliferative lesions were either myeloid dysplasia or myeloid leukemia (overall, 12%). The mean age of wild-type mice with neoplasms is 22 months (Figure 3). As described before,[31,32] *PARP-1*-null mice develop few pathological phenotypes by 24 months of age. Only 2 animals of 18 analyzed developed a neoplasm (Table 1). One *PARP-1*-null mouse had an hepatocellular carcinoma at ~18 months of age and one

PARP-1 mutant had developed a myeloid hyperplasia at 11 months of age. No statistical analysis was performed with this cohort (Figure 3).

Wrn$^{\Delta hel/\Delta hel}$ mutant mice were remarkable with respect to the variety of neoplasms they developed compared to wild-type animals (Table 1). Approximately, 45% of *Wrn*$^{\Delta hel/\Delta hel}$ mutant mice developed some types of neoplasm compared to 27% for wild-type mice and this difference was statistically significant (Table 1). Interestingly, *PARP-1*-null/*Wrn*$^{\Delta hel/\Delta hel}$ mice developed the same type of neoplasms as *Wrn*$^{\Delta hel/\Delta hel}$ mutant mice (Table 1). Approximately, 47% of *PARP-1*-null/*Wrn*$^{\Delta hel/\Delta hel}$ mice developed a neoplasm. Thus, *PARP-1*-null/*Wrn*$^{\Delta hel/\Delta hel}$ mice are not more cancer prone than *Wrn*$^{\Delta hel/\Delta hel}$ animals. However, these mice developed their neoplasms at a younger age than *Wrn*$^{\Delta hel/\Delta hel}$ mutant animals. The mean age of *PARP-1*-null/*Wrn*$^{\Delta hel/\Delta hel}$ mice with neoplasms is 14 months (Figure 3). Moreover, 18% of *PARP-1*-null/*Wrn*$^{\Delta hel/\Delta hel}$ mice developed more than two types of neoplasm, simultaneously. Only 9% of *Wrn*$^{\Delta hel/\Delta hel}$ mice developed more than two types of neoplasms. This difference between both cohorts is significant (chi-square test; $P < 0.05$ in Table 1). Finally, the difference between the mean age of *Wrn*$^{\Delta hel/\Delta hel}$ and *PARP-1*-null/*Wrn*$^{\Delta hel/\Delta hel}$ animals with neoplasms is significant (Figure 3; analysis of variance, $P < 0.05$). All these results suggest that a defect in the *PARP-1* gene product accelerates the cancer phenotype seen in the *Wrn* mutant mice.

Analysis of Mutant MEFs

Because reduced growth rate and premature senescence are properties generally associated with the premature aging of human WS fibroblasts,[44] we examined this property in fibroblasts derived from *PARP-1*-null/*Wrn*$^{\Delta hel/\Delta hel}$ mice. MEFs from three embryos of each genotype were established as described previously.[11] Previous data have indicated that *Wrn*$^{\Delta hel/\Delta hel}$ mutant and *PARP-1*-null cell lines acquired a slower growth rate than wild-type cell lines with the number of passage in culture.[11,31] Interestingly, *PARP-1*-null/*Wrn*$^{\Delta hel/\Delta hel}$ MEFs already had a slow growth phenotype at the first passage (approximately five population doublings) in culture compared to cells of all other genotype. After the second passage in culture, it could take up to 8 weeks for the *PARP-1*-null/*Wrn*$^{\Delta hel/\Delta hel}$ MEFs to reach confluence. They stopped growing by the third passage (after ~15 to 20 population doublings) in culture. At that point, such cultures could be maintained for several months without any evidence of cell division. Thus, in contrast to the other MEFs that are still growing after the 15 to 20 population doublings in culture, *PARP-1*-null/*Wrn*$^{\Delta hel/\Delta hel}$ MEFs senesce very rapidly. An example of growth curves is given in Figure 4 for MEFs of each genotype after the third passage in culture. Finally, fluorescence-activated cell sorting analyses have indicated that *Wrn*$^{\Delta hel/\Delta hel}$, *PARP-1*-null, and *PARP-1*-null/*Wrn*$^{\Delta hel/\Delta hel}$ MEFs did not exhibit a significant increase in their apoptotic fraction with the number of passages in culture compared to wild-type cells (data not shown).

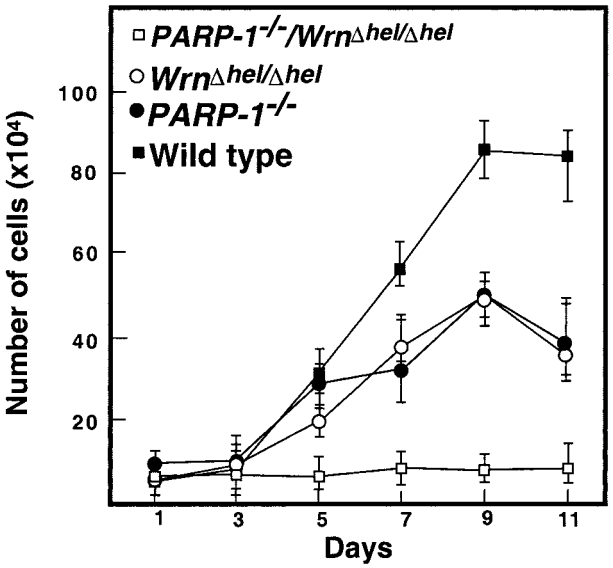

Figure 4. Differential growth properties of MEFs after the third passage in culture. Cells from wild-type, *Wrn*$^{\Delta hel/\Delta hel}$, *PARP-1*-null, and *PARP-1*-null/*Wrn*$^{\Delta hel/\Delta hel}$ mutant embryos were plated and counted as described in Materials and Methods. Each **curve** represents MEFs from three different embryos (from different litters) for each genotype.

Increased Genomic Instability in Mutant MEFs

Chromosome analyses were performed on MEFs of all four genotypes to determine the chromosome composition of the cells at the beginning of the culture. There is an increase in aneuploidy with the number of population doubling in culture for all of the MEFs analyzed. However, as indicated in Table 2, aneuploidy was already high for the *Wrn*$^{\Delta hel/\Delta hel}$, the *PARP-1*-null, and the *PARP-1*-null/*Wrn*$^{\Delta hel/\Delta hel}$ MEFs compared to wild-type cells. After 5 to 10 population doublings, more than 70% of wild-type metaphase spreads exhibited a diploid content. In contrast, less than 50% of the metaphase spreads from the *Wrn*$^{\Delta hel/\Delta hel}$, the *PARP-1*-null, and the *PARP-1*-null/*Wrn*$^{\Delta hel/\Delta hel}$ MEFs were diploid by the 10th population doubling. The differences between wild-type and every mutant MEFs at 5 to 10 population doublings were statistically significant (chi-square test; $P < 0.005$ or $P < 0.001$ in Table 2). These results indicate that MEFs with a mutation either in the *PARP-1*, the *Wrn,* or both genes reached a high degree of aneuploidy within fewer cell divisions when compared to wild-type cells.

Detailed cytogenetic analysis (Table 3) revealed all kinds of chromosomal abnormalities in the mutant cells, such as fragmentation, breaks, and end-to-end fusions including Robertsonian-like configurations, dicentric, and ring chromosomes (Figure 5). The sum of all chromosomal abnormalities was always the highest in *PARP-1*-null/*Wrn*$^{\Delta hel/\Delta hel}$ MEFs even early on in cultures (top part of Table 3). The numbers of end-to-end fusions were similar between the *Wrn*$^{\Delta hel/\Delta hel}$, the *PARP-1*-null, and the *PARP-1*-null/*Wrn*$^{\Delta hel/\Delta hel}$ MEFs (Table 3) even after 10 population doublings. However, the number of chromatid breaks was strikingly higher in the *PARP-1*-null/*Wrn*$^{\Delta hel/\Delta hel}$ MEFs. An average of 1.17 fragment per metaphase was detected in these cells after only 10 population dou-

Table 2. Effect of Wrn and/or PARP-1 Deficiency on Chromosome Number

Genotype	Population doublings	Mean % of*			*P* value†
		Diploid cells	Tetraploid cells	Aneuploid cells	
Wild type	5–10	71	8	21	—
Wrn$^{\Delta hel/\Delta hel}$	5–10	45	16	39	<0.001
Parp-1$^{-/-}$	5–10	51	12	37	<0.005
Parp-1$^{-/-}$/*Wrn*$^{\Delta hel/\Delta hel}$	5–10	44	7	49	<0.001

*For each genotype, the mean percentage is calculated from a total of 200 cells from different cultures derived from three embryos.
†Chi-square tests comparing wild-type mice to mutant mice that are significant.

blings. In contrast, an average of 0.02 fragment per metaphase was detected in wild-type cells after 10 population doublings. For the *PARP-1*-null and the *Wrn*$^{\Delta hel/\Delta hel}$ MEFs, 0.22 and 0.09 fragment per metaphase, respectively, was detected after more than 15 population doublings. The difference between *PARP-1*-null/*Wrn*$^{\Delta hel/\Delta hel}$ MEFs and either *PARP-1*-null or *Wrn*$^{\Delta hel/\Delta hel}$ cells is statistically significant (*t*-test, $P < 0.0005$). Triradial and quadriradial structures caused by chromatid translocations and double-minutes structure were also more frequent in *PARP-1*-null/*Wrn*$^{\Delta hel/\Delta hel}$ cells (Table 3). Importantly, these observations were always similar for all embryos of a specific genotype. Examples of chromosomal rearrangements from *PARP-1*-null/*Wrn*$^{\Delta hel/\Delta hel}$ cells are given in Figure 5. All these observations indicate that in addition to the rapid increase in aneuploidy, there is also a rapid increase in the extent of chromosomal rearrangements in cells lacking both PARP-1 and Wrn helicase activities. This overall increase in genomic instability is likely to affect the *PARP-1*-null/*Wrn*$^{\Delta hel/\Delta hel}$ cell growth.

Telomere Instability in Mutant MEFs

Telomeres are DNA structures composed of TTAGGG repeats required for the maintenance of chromosomal ends. They protect chromosomes from end-to-end fusion, recombination, and degradation. It is known that replicative decline of somatic cells is associated with loss of telomeric repeats.[45,46] To determine whether loss of telomere length is responsible for the rapid senescence observed with the *PARP-1*-null/*Wrn*$^{\Delta hel/\Delta hel}$ MEFs, telomeric sequences were analyzed by semiquantitative primed *in situ* labeling (Figure 5I). The analyses were performed on metaphase spreads from *PARP-1*-null/*Wrn*$^{\Delta hel/\Delta hel}$ cells one passage before the senescence phenotype (at the 10th or 12th population doubling). These samples were compared to metaphase spreads from wild-type, *Wrn*$^{\Delta hel/\Delta hel}$, and *PARP-1*-null cells at exactly the same population doubling. As described previously, *PARP-1*-null MEFs exhibit shorter telomeres compared to wild-type cells.[33] The mean value of telomere fluorescence for the *PARP-1*-null cell is 53% of that of the wild-type cells (Figure 6). *Wrn*$^{\Delta hel/\Delta hel}$ MEFs also exhibit shorter telomeres than wild-type cells. Surprisingly, even though *PARP-1*-null/*Wrn*$^{\Delta hel/\Delta hel}$ MEFs senesce more rapidly than *PARP-1*-null or *Wrn*$^{\Delta hel/\Delta hel}$ cells, their mean value of telomere fluorescence is similar to the *Wrn*$^{\Delta hel/\Delta hel}$ fibroblasts (Figure 6). The mean values of telomere fluorescence for both the *Wrn*$^{\Delta hel/\Delta hel}$ and the *PARP-1*-null/*Wrn*$^{\Delta hel/\Delta hel}$ MEFs are ~60 to 70% of that of the wild-type cells, respectively. Finally, telomerase activity was examined by using the telomere repeat amplification protocol assay. The levels of telomerase activity were the same in all of the MEFs examined (data not shown). Thus, a simple deletion in the helicase domain of the mouse Wrn protein affects the length of the telomeres. However, the results also indicate that the altered length of the telomeres seen in the *PARP-1*-null/*Wrn*$^{\Delta hel/\Delta hel}$ MEFs is not the only explanation for their abrupt arrest in cell growth.

Discussion

The WRN protein is known to interact with several proteins associated with the DNA replication complex.[17]

Table 3. Effect of Wrn and/or PARP-1 Deficiency on Chromosome Integrity

Genotype	Number of metaphases analyzed/ karyotyped	Population doublings	Total number of structural chromosome aberrations					
			End-to-end fusions	Fragments	Fragment/ metaphase	Mar	DMs	TR/QR
Wild type	100/15	5–10	0	2 (2 CT)	0.02	0		
Wrn$^{\Delta hel/\Delta hel}$	150/30	5–10	18 (14 RL, 4 DIC)	15 (2 CT, 5 AC, 8 CF)	0.10	21		
Parp-1$^{-/-}$	150/30	5–10	14 (6 RL, 5 DIC, 3 RN)	43 (31 CT, 1CH, 11ACF)	0.29	36		
Parp-1$^{-/-}$/*Wrn*$^{\Delta hel/\Delta hel}$	150/30	5–10	31 (26 RL, 3 DIC, 2 RN)	57 (32 CT, 7 CH, 5 AC, 13 CF)	0.38	30	4	
Wild type	100/15	15–20	2 (2RL)	0	0	0		
Wrn$^{\Delta hel/\Delta hel}$	150/30	15–20	12 (9 RL, 1 DIC, 2 RN)	13 (3 CT, 1 AC, 6 CF)	0.09	17	2	
Parp-1$^{-/-}$	150/30	15–20	16 (13 RL, 3 RN)	33 (23 CT, 5 AC, 5 CF)	0.22	32		1
Parp-1$^{-/-}$/*Wrn*$^{\Delta hel/\Delta hel}$	150/30	10–15	15 (9 RL, 4 DIC, 2 RN)	175 (131 CT, 14 CH, 18 AC, 12 CF)	1.17*	46	14	11

RL, Robertsonian-like configurations; DIC, dicentric chromosomes; RN, ring-like chromosomes; CT, chromatid breaks; CH, chromosome breaks; AC, acentric chromosomal fragments; CF, centric chromosomal fragments; Mar, marker chromosome; DMs, double minute structure; TR/QR, triradial or quadriradial structures.
*The difference between *Parp-1*$^{-/-}$/*Wrn*$^{\Delta hel/\Delta hel}$ and *Wrn*$^{\Delta hel/\Delta hel}$ or *Parp-1*$^{-/-}$ is statistically significant, $P < 0.0005$.

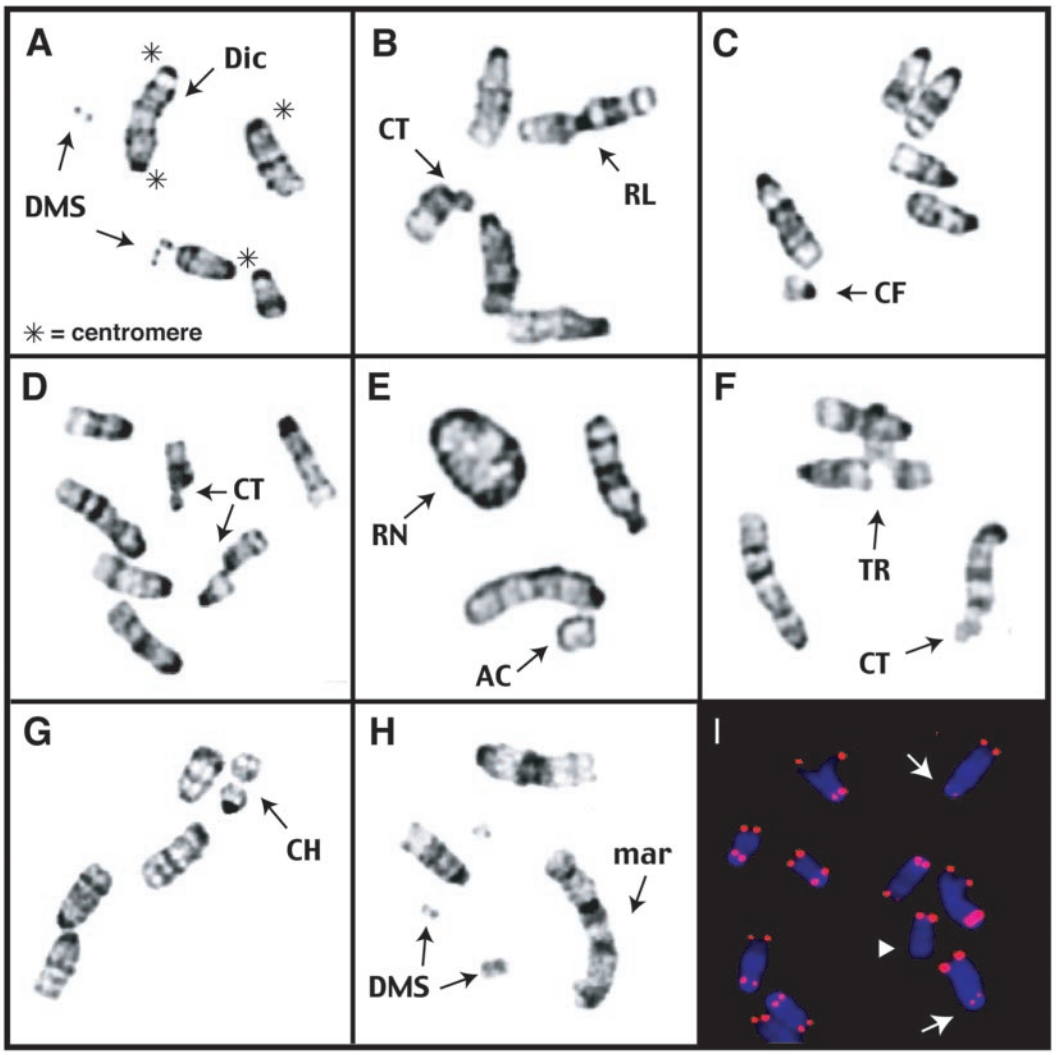

Figure 5. Examples of partial metaphases from *PARP-1*-null/*Wrn*$^{\Delta bel/\Delta bel}$ MEFs. **A–H:** Chromosomal abnormalities found after GTW-banding analysis. **I:** Telomere fluorescence analysis using primed *in situ* labeling. Abnormalities are dicentric chromosome (Dic), double-minute structures (DMs), chromatid breaks (CT), Robertsonian-like translocation (RL), centric chromosomal fragment (CF), ring chromosome (RN), acentric chromosomal fragment (AC), a triradial structure caused by chromatid translocation (TR), chromosomal break (CH) and marker chromosome (Mar). In I, the **arrows** point to short telomeres as illustrated by the low intensity of the rhodamine (red) signals on the sister chromatids.

PARP-1 is also an enzyme that co-purifies with the DNA replication complex.[19] Because both proteins are associated with the DNA replication complex and both proteins are involved in some types of DNA repair, it was thus reasonable to look at a possible interaction between these proteins *in vivo*. Indeed, co-immunoprecipitation experiments have indicated a close association of WRN and PARP-1 in human cells. Past preliminary immunoprecipitation experiments did not reveal an interaction between the PARP-1 and WRN enzymes because of the antibodies used.[47] This study indicates that co-immunoprecipitation of WRN and PARP-1 proteins are detected only with specific antibodies to the C-terminus region of PARP-1 or the N-terminus region of WRN. Preliminary *in vitro* binding data have indicated that an N-terminus region of the PARP-1 enzyme interacts directly with a C-terminus region of the WRN protein (unpublished data). Antibodies against epitopes on the C-terminus portion of WRN may interfere with this interaction. Additional experiments are required to identify the exact amino acid residues involved in this interaction. The exact functional effect of PARP-1 on WRN exonuclease/helicase activities is currently under investigation.

Neoplasm Formation in Wrn$^{\Delta hel/\Delta hel}$ *and PARP-1-Null/Wrn*$^{\Delta hel/\Delta hel}$ *Mice*

Several different neoplasms and other pathological findings were observed in *Wrn*$^{\Delta hel/\Delta hel}$ mutant mice older than 18 months of age. It was found that ~80% of the mice had developed some types of disease including hyperplasias or neoplasms in one of their organs by 24 months of age.[36] Interestingly, the *PARP-1*-null/*Wrn*$^{\Delta hel/\Delta hel}$ developed similar types of neoplasms but at a younger age when compared to *Wrn*$^{\Delta hel/\Delta hel}$ animals. It is possible that the onset of the pathologies is the same between *Wrn*$^{\Delta hel/\Delta hel}$ and *PARP-1*-null/*Wrn*$^{\Delta hel/\Delta hel}$ animals, but the evolution of

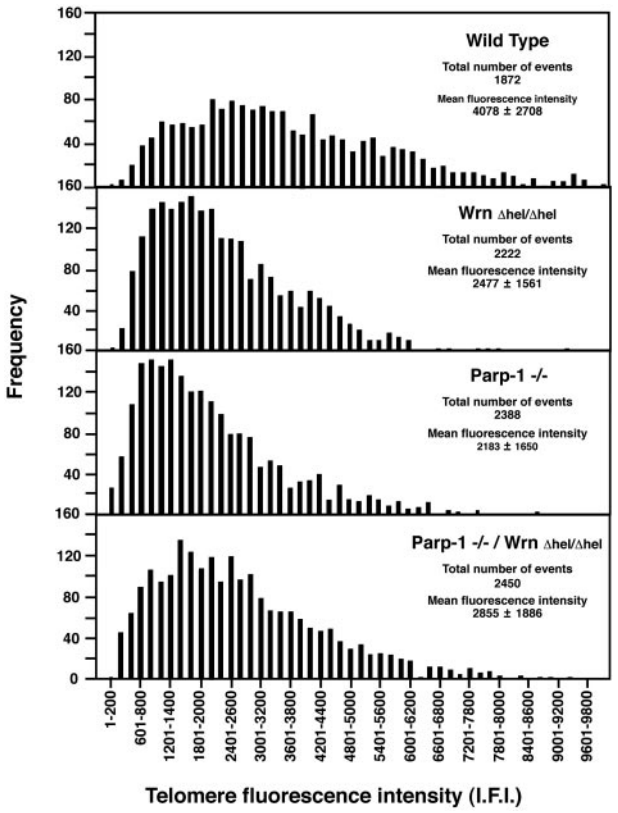

Figure 6. Primed *in situ* labeling analyses of telomere length in wild-type, *Wrn*$^{\Delta hel/\Delta hel}$, *PARP-1*-null, and *PARP-1*-null/*Wrn*$^{\Delta hel/\Delta hel}$ MEFs. Frequency distributions of telomere fluorescence values (pooled p- and q-arm values) in metaphase chromosomes from MEFs with the indicated genotype are shown. The *x* axis depicts the rhodamine-integrated fluorescence intensity (I.F.I.) values for telomeres from sister chromatids; the *y* axis shows the frequency of telomeres of a given fluorescence intensity value.

the pathologies is faster in *PARP-1*-null/*Wrn*$^{\Delta hel/\Delta hel}$ mice. Under such conditions, *PARP-1*-null/*Wrn*$^{\Delta hel/\Delta hel}$ mice appear sick sooner than *Wrn*$^{\Delta hel/\Delta hel}$ animals. Thus, it is concluded that a defect in the *PARP-1* gene product accelerates the phenotype seen in the *Wrn* mutant mice.

It has been previously reported that a stable mutant Wrn protein is synthesized from the *Wrn*$^{\Delta hel/\Delta hel}$ mice used in this study.[11,16] However, this mutant protein does not co-purify with the DNA replication complex[16] indicating that the deletion will affect the three-dimensional structure of the whole protein and probably protein-protein interactions *in vivo*. Nonetheless, we cannot rule out the possibility that this mutant Wrn protein can interact and disrupt the function of other protein complexes involved in genomic stability. This is even more so as a *Wrn*-null mutation in mouse, which mimics the mutations seen in WS patients, does not reiterate all of the phenotypes described for our *Wrn*$^{\Delta hel/\Delta hel}$ mice.[48] Importantly, our mutant mice synthesize a stable mutant protein with an intact exonuclease domain that may have abnormal activity affecting genomic stability. Purification and analysis of this mutant Wrn protein is currently under investigation to determine whether it has any functional exonuclease activity. Finally, although *Wrn*$^{\Delta hel/\Delta hel}$ mice demonstrate a complex phenotype, they do not recapitulate all of the symptoms described for WS patients. As such, *Wrn*$^{\Delta hel/\Delta hel}$ may not be a good model for WS. Nevertheless, our results clearly indicate that a mutation in the helicase domain of the Wrn protein will affect genomic stability.

Interestingly, *PARP-1*-null MEFs and *Wrn*$^{\Delta hel/\Delta hel}$ cells showed similar strong karyotypic instability *in vitro* and yet *PARP-1*-null mice did not develop neoplasms like the *Wrn*$^{\Delta hel/\Delta hel}$ animals. Preliminary karyotype analyses have indicated that there are some chromosomal rearrangements that can be detected in several *PARP-1*-null MEFs cultures that are different from those observed in either *Wrn*$^{\Delta hel/\Delta hel}$ or *PARP-1*-null/*Wrn*$^{\Delta hel/\Delta hel}$ cells. These preliminary analyses indicate that different sets of genes are mutated in cells of all three genotypes. Such differences in the spectrum of genomic mutation may be responsible for the different outcome observed *in vivo* for each genotype. Thorough spectral karyotyping analyses and comparative genomic hybridization experiments are underway to test this possibility.

Increased Gnomic Instability and Proliferative Decline in PARP-1-Null/Wrn$^{\Delta hel/\Delta hel}$ *MEFs*

It is known that replicative decline of somatic cells is associated with a loss of telomeric repeats and that short telomeres contribute to chromosomal instability in cells.[45,46] All mutant MEFs exhibit a decrease in their telomere length compared to wild-type cells. Shorter telomeres might have caused the mutant cells to acquire a slow growth phenotype. However, the proportion of *PARP-1*-null/*Wrn*$^{\Delta hel/\Delta hel}$ chromosomes with very short telomeres is not greater than those from the *Wrn*$^{\Delta hel/\Delta hel}$ or *PARP-1*-null cells, even though *PARP-1*-null/*Wrn*$^{\Delta hel/\Delta hel}$ proliferation declines more rapidly than the other genotypes in culture. *PARP-1*-null/*Wrn*$^{\Delta hel/\Delta hel}$ MEFs are remarkable for the number of metaphase spreads with chromatid breaks, triradial or quadriradial structures, and double-minute chromosomes compared to wild-type, *Wrn*$^{\Delta hel/\Delta hel}$, or *PARP-1*-null cells. From these results, it is concluded that it is the higher frequency of chromosomal fragments and the higher frequency of chromosomal breaks that are the major contributors of the observed abrupt cell-growth arrest in the *PARP-1*-null/*Wrn*$^{\Delta hel/\Delta hel}$ culture.

Possible Function of Wrn and PARP-1 at DNA Replication Forks

PARP-1 is a nick sensor that also recognizes and binds to double-strand breaks. It facilitates DNA repair by protecting against uncontrolled DNA recombination.[48] In addition to its anti-recombinogenic effect, PARP-1 is believed to be part of a DNA break-signaling mechanism recruiting and regulating DNA repair molecules at the sites of DNA damage.[48,49] It has been shown that PARP-1-deficient MEFs have a prolonged delay in DNA strand-break resealing leading to chromosomal instability.[50] PARP-1 is also believed to participate in the base excision repair pathway.[21,22] There is no direct evidence for the participation of WRN in base excision repair. However, WS cells are sensitive to the drug 4-nitroquinoline 1-oxide.[51] This

agent will cause alkylation of DNA and induce oxidative stress in cells.[52] Hence, there is the interesting possibility that the WRN protein might be involved in the efficient removal of certain DNA lesions by a base excision repair pathway. In addition, WRN interacts with Fen1 and proliferation cellular nuclear antigen,[16,18] both of which are involved in base excision repair.[53] Future experiments should yield insight in the potential involvement of WRN in base excision repair of specific oxidative lesions.

The WRN homologues are considered suppressors of illegitimate recombination. Thus, one possible function of the mouse Wrn protein is to monitor recombinational repair of double-strand breaks at the site of DNA replication.[17] Aberrant DNA structures may arise during the process of DNA replication causing collapses of replication forks. Such collapses would generate regions of DNA breaks that may provide substrates for the initiation of recombination. If the Wrn protein is mutated, illegitimate recombination may occur at a high frequency generating abnormal chromosomes as it is observed in our $Wrn^{\Delta hel/\Delta hel}$ mice.

Finally, several chromatid and chromosomal breaks were detected in PARP-1-null/$Wrn^{\Delta hel/\Delta hel}$ MEFs metaphase spreads and such DNA breaks persisted in these cells apparently generating chromosomal fragmentation (Figure 5 and Table 3). In comparison, fewer persistent breaks were detected in $Wrn^{\Delta hel/\Delta hel}$ and *PARP-1*-null karyotypes. These results suggest that PARP-1 and Wrn proteins are involved together in the processing of DNA breaks not only during DNA replication, but also after the S phase of the cell cycle.

With respect to DNA damaging agents, it is interesting to note that PARP-1 activity is required for rapid accumulation of p53, activation of p53 sequence-specific DNA binding, and its transcriptional activity after DNA damage.[54] The p53 tumor suppressor is required for G_1 arrest[55] and it is believed that this arrest allows cells time to repair DNA damage before being fixed as mutations. A portion of this p53-dependent cell-cycle control is manifest via p21 induction which is, in turn, responsible for the G_1/S cell-cycle checkpoint.[37] In addition to cell-cycle arrest, the ability of p53 to induce apoptosis is thought to be an important factor for its tumor suppressor function.[56] It has been shown that human WS cells have an attenuation of the *p53*-dependent apoptotic pathway.[57] Moreover, a role for WRN in transcription is also suggested by the observation that overexpression of WRN results in enhanced p53-dependent transcriptional activity.[58] Consequently, a suboptimal activation of p53 in cells accumulating DNA breaks, as it is observed in *PARP-1*-null/$Wrn^{\Delta hel/\Delta hel}$ cells, would certainly affect cell proliferation. Finally, several *PARP-1*-null/$Wrn^{\Delta hel/\Delta hel}$ metaphase spreads have shown rearrangements of the region of chromosome 12 containing the *p53* gene. Careful analysis of p53 status in all our MEFs is thus required.

Acknowledgments

We thank Dr. P. Leder (Harvard Medical School, Boston, MA) and Dr. E. F. Wagner (Research Institute of Molecular Pathology, Vienna, Austria) for the $Wrn^{\Delta hel/\Delta hel}$ and the *PARP-1*-null mice, respectively; Dr. E. A. Drobetsky for careful editing of the manuscript and helpful comments; A. Julien for technical assistance with the animals; and Dr. L. Turcot-Lemay for the statistical analyses.

References

1. Goto M, Miller RW, Ishikawa Y, Sugano H: Excess of rare cancers in Werner syndrome (adult progeria). Cancer Epidemiol Biomarkers Prev 1996, 5:239–246
2. Yu CE, Oshima J, Fu YH, Wijsman EM, Hisama F, Alish R, Matthews S, Nakura J, Miki T, Quais S, Martin GM, Mulligan J, Schellenberg GD: Positional cloning of the Werner's syndrome gene. Science 1996, 272:258–262
3. Huang S, Beresten S, Li B, Oshima J, Ellis NA, Campisi J: Characterization of the human and mouse WRN 3′–>5′ exonuclease. Nucleic Acids Res 2000, 28:2396–2405
4. Kamath-Loeb AS, Shen JC, Loeb LA, Fry M: Werner syndrome protein. II. Characterization of the integral 3′–> 5′ DNA exonuclease. J Biol Chem 1998, 273:34145–34150
5. Shen JC, Gray MD, Oshima J, Kamath-Loeb AS, Fry M, Loeb LA: Werner syndrome protein. I. DNA helicase and DNA exonuclease reside on the same polypeptide. J Biol Chem 1998, 273:34139–34144
6. Scappaticci S, Forabosco A, Borroni G, Orecchia G, Fraccaro M: Clonal structural chromosomal rearrangements in lymphocytes of four patients with Werner's syndrome. Ann Genet 1990, 33:5–8
7. Schonberg S, Niermeijer MF, Bootsma D, Henderson E, German J: Werner's syndrome: proliferation in vitro of clones of cells bearing chromosome translocations. Am J Hum Genet 1984, 36:387–397
8. Hoehn H, Bryant EM, Au K, Norwood TH, Boman H, Martin GM: Variegated translocation mosaicism in human skin fibroblast cultures. Cytogenet Cell Genet 1975, 15:282–298
9. Schulz VP, Zakian VA, Ogburn CE, McKay J, Jarzebowicz AA, Edland SD, Martin GM: Accelerated loss of telomeric repeats may not explain accelerated replicative decline of Werner syndrome cells. Hum Genet 1996, 97:750–754
10. Tahara H, Tokutake Y, Maeda S, Kataoka H, Watanabe T, Satoh M, Matsumoto T, Sugawara M, Ide T, Goto M, Furuichi Y, Sugimoto M: Abnormal telomere dynamics of B-lymphoblastoid cell strains from Werner's syndrome patients transformed by Epstein-Barr virus. Oncogene 1997, 15:1911–1920
11. Lebel M, Leder P: A deletion within the murine Werner syndrome helicase induces sensitivity to inhibitors of topoisomerase and loss of cellular proliferative capacity. Proc Natl Acad Sci USA 1998, 95:13097–13102
12. Takeuchi F, Hanaoka F, Goto M, Yamada M, Miyamoto T: Prolongation of S phase and whole cell cycle in Werner's syndrome fibroblasts. Exp Gerontol 1982, 17:473–480
13. Poot M, Hoehn H, Runger TM, Martin GM: Impaired S-phase transit of Werner syndrome cells expressed in lymphoblastoid cell lines. Exp Cell Res 1992, 202:267–273
14. Fujiwara Y, Kano Y, Ichihashi M, Nakao Y, Matsumura T: Abnormal fibroblast aging and DNA replication in the Werner syndrome. Adv Exp Med Biol 1985, 190:459–477
15. Hanaoka F, Yamada M, Takeuchi F, Goto M, Miyamoto T, Hori T: Autoradiographic studies of DNA replication in Werner's syndrome cells. Adv Exp Med Biol 1985, 190:439–457
16. Lebel M, Spillare EA, Harris CC, Leder P: The Werner syndrome gene product co-purifies with the DNA replication complex and interacts with PCNA and topoisomerase I. J Biol Chem 1999, 274:37795–37799
17. Lebel M: Werner syndrome: genetic and molecular basis of a premature aging disorder. Cell Mol Life Sci 2001, 58:857–867
18. Brosh Jr RM, von Kobbe C, Sommers JA, Karmakar P, Opresko PL, Piotrowski J, Dianova I, Dianov GL, Bohr VA: Werner syndrome protein interacts with human flap endonuclease 1 and stimulates its cleavage activity. EMBO J 2001, 20:5791–5801
19. Simbulan-Rosenthal CM, Rosenthal DS, Hilz H, Hickey R, Malkas L, Applegren N, Wu Y, Bers G, Smulson ME: The expression of poly-

(ADP-ribose) polymerase during differentiation-linked DNA replication reveals that it is a component of the multiprotein DNA replication complex. Biochemistry 1996, 35:11622–11633
20. Dantzer F, Nasheuer HP, Vonesch JL, de Murcia G, Menissier-de Murcia J: Functional association of poly(ADP-ribose) polymerase with DNA polymerase alpha-primase complex: a link between DNA strand break detection and DNA replication. Nucleic Acids Res 1998, 26: 1891–1898
21. Burkle A: Physiology and pathophysiology of poly(ADP-ribosyl)ation. Bioessays 2001, 23:795–806
22. Le Rhun Y, Kirkland JB, Shah GM: Cellular responses to DNA damage in the absence of Poly(ADP-ribose) polymerase. Biochem Biophys Res Commun 1998, 245:1–10
23. Schreiber V, Ame JC, Dolle P, Schultz I, Rinaldi B, Fraulob V, Menissier-de Murcia J, de Murcia G: Poly(ADP-ribose) polymerase-2 (PARP-2) is required for efficient base excision DNA repair in association with PARP-1 and XRCC1. J Biol Chem 2002, 277:23028–23036
24. Masson M, Niedergang C, Schreiber V, Muller S, Menissier-de Murcia J, de Murcia G: XRCC1 is specifically associated with poly(ADP-ribose) polymerase and negatively regulates its activity following DNA damage. Mol Cell Biol 1998, 18:3563–3571
25. Meyer R, Muller M, Beneke S, Kupper JH, Burkle A: Negative regulation of alkylation-induced sister-chromatid exchange by poly(ADP-ribose) polymerase-1 activity. Int J Cancer 2000, 88:351–355
26. Masutani M, Nozaki T, Nakamoto K, Nakagama H, Suzuki H, Kusuoka O, Tsutsumi M, Sugimura T: The response of Parp knockout mice against DNA damaging agents. Mutat Res 2000, 462:159–166
27. Ménissier de Murcia J, Niedergang C, Trucco C, Ricoul M, Dutrillaux B, Mark M, Oliver FJ, Masson M, Dierich A, LeMeur M, Walztinger C, Chambon P, de Murcia G: Requirement of poly(ADP-ribose) polymerase in recovery from DNA damage in mice and in cells. Proc Natl Acad Sci USA 1997, 94:7303–7307
28. Tsutsumi M, Masutani M, Nozaki T, Kusuoka O, Tsujiuchi T, Nakagama H, Suzuki H, Konishi Y, Sugimura T: Increased susceptibility of poly(ADP-ribose) polymerase-1 knockout mice to nitrosamine carcinogenicity. Carcinogenesis 2001, 22:1–3
29. Beneke R, Moroy T: Inhibition of poly(ADP-ribose) polymerase activity accelerates T-cell lymphomagenesis in p53 deficient mice. Oncogene 2001, 20:8136–8141
30. Tong WM, Hande MP, Lansdorp PM, Wang ZQ: DNA strand break-sensing molecule poly(ADP-Ribose) polymerase cooperates with p53 in telomere function, chromosome stability, and tumor suppression. Mol Cell Biol 2001, 21:4046–4054
31. Wang ZQ, Auer B, Stingl L, Berghammer H, Haidacher D, Schweiger M, Wagner EF: Mice lacking ADPRT and poly(ADP-ribosyl)ation develop normally but are susceptible to skin disease. Genes Dev 1995, 9:509–520
32. Wang ZQ, Stingl L, Morrison C, Jantsch M, Los M, Schulze-Osthoff K, Wagner EF: PARP is important for genomic stability but dispensable in apoptosis. Genes Dev 1997, 11:2347–2358
33. d'Adda di Fagagna F, Hande MP, Tong WM, Lansdorp PM, Wang ZQ, Jackson SP: Functions of poly(ADP-ribose) polymerase in controlling telomere length and chromosomal stability. Nat Genet 1999, 23: 76–80
34. Samper E, Goytisolo FA, Menissier-de Murcia J, Gonzalez-Suarez E, Cigudosa JC, de Murcia G, Blasco MA: Normal telomere length and chromosomal end capping in poly(ADP-ribose) polymerase-deficient mice and primary cells despite increased chromosomal instability. J Cell Biol 2001, 154:49–60
35. Simbulan-Rosenthal CM, Ly DH, Rosenthal DS, Konopka G, Luo R, Wang ZQ, Schultz PG, Smulson ME: Misregulation of gene expression in primary fibroblasts lacking poly(ADP-ribose) polymerase. Proc Natl Acad Sci USA 2000, 97:11274–11279
36. Lebel M, Cardiff RD, Leder P: Tumorigenic effect of nonfunctional p53 or p21 in mice mutant in the Werner syndrome helicase. Cancer Res 2001, 61:1816–1819
37. Deng C, Zhang P, Harper JW, Elledge SJ, Leder P: Mice lacking p21CIP1/WAF1 undergo normal development, but are defective in G1 checkpoint control. Cell 1995, 82:675–684
38. Drouin R, Lemieux N, Richer CL: High-resolution R-banding at the 1250-band level. 1. Technical considerations on cell synchronization and R-banding (RHG and RBG). Cytobios 1988, 56:107–125
39. Cowell JK: A photographic representation of the variability in the G-banded structure of the chromosomes in the mouse karyotype. A guide to the identification of the individual chromosomes. Chromosoma 1984, 89:294–320
40. Krejci K, Koch J: Improved detection and comparative sizing of human chromosomal telomeres in situ. Chromosoma 1998, 107:198–203
41. Russo A, Priante G, Tommasi AM: PRINS localization of centromeres and telomeres in micronuclei indicates that in mouse splenocytes chromatid non-disjunction is a major mechanism of aneuploidy. Mutat Res 1996, 372:173–180
42. Therkelsen AJ, Nielsen A, Koch J, Hindjaer J, Kolvraa S: Staining of human telomeres with primed in situ labeling (PRINS). Cytogenet Cell Genet 1995, 68:115–118
43. Lansdorp PM, Verwoerd NP, van de Rijke FM, Dragowska V, Little MT, Dirks RW, Raap AK, Tanke HJ: Heterogeneity in telomere length of human chromosomes. Hum Mol Genet 1996, 5:685–691
44. Salk D, Bryant E, Au K, Hoehn H, Martin GM: Systematic growth studies, cocultivation, and cell hybridization studies of Werner syndrome cultured skin fibroblasts. Hum Genet 1981, 58:310–316
45. Greider CW: Telomere length regulation. Annu Rev Biochem 1996, 65:337–365
46. Martin GM: Genetic and environmental modulations of chromosomal stability: their roles in aging and oncogenesis. Ann NY Acad Sci 1991, 621:401–417
47. Lebel M: Increased frequency of DNA deletions in pink-eyed unstable mice carrying a mutation in the Werner syndrome gene homologue. Carcinogenesis 2002, 23:213–216
48. Chatterjee S, Berger SJ, Berger NA: Poly(ADP-ribose) polymerase: a guardian of the genome that facilitates DNA repair by protecting against DNA recombination. Mol Cell Biochem 1999, 193:23–30
49. Althaus FR, Kleczkowska HE, Malanga M, Muntener CR, Pleschke JM, Ebner M, Auer B: Poly ADP-ribosylation: a DNA break signal mechanism. Mol Cell Biochem 1999, 193:5–11
50. Trucco C, Oliver FJ, de Murcia G, Menissier-de Murcia J: DNA repair defect in poly(ADP-ribose) polymerase-deficient cell lines. Nucleic Acids Res 1998, 26:2644–2649
51. Ogburn CE, Oshima J, Poot M, Chen R, Hunt KE, Gollahon KA, Rabinovitch PS, Martin GM: An apoptosis-inducing genotoxin differentiates heterozygotic carriers for Werner helicase mutations from wild-type and homozygous mutants. Hum Genet 1997, 101:121–125
52. Nunoshiba T, Demple B: Potent intracellular oxidative stress exerted by the carcinogen 4-nitroquinoline-N-oxide. Cancer Res 1993, 53: 3250–3252
53. Matsumoto Y: Molecular mechanism of PCNA-dependent base excision repair. Prog Nucleic Acid Res Mol Biol 2001, 68:129–138
54. Wang X, Ohnishi K, Takahashi A, Ohnishi T: Poly(ADP-ribosyl)ation is required for p53-dependent signal transduction induced by radiation. Oncogene 1998, 17:2819–2825
55. Kuerbitz SJ, Plunkett BS, Walsh WV, Kastan MB: Wild-type p53 is a cell cycle checkpoint determinant following irradiation. Proc Natl Acad Sci USA 1992, 89:7491–7495
56. Levine AJ: p53, the cellular gatekeeper for growth and division. Cell 1997, 88:323–331
57. Spillare EA, Robles AI, Wang XW, Shen JC, Yu CE, Schellenberg GD, Harris CC: p53-mediated apoptosis is attenuated in Werner syndrome cells. Genes Dev 1999, 13:1355–1356
58. Blander G, Kipnis J, Leal JF, Yu CE, Schellenberg GD, Oren M: Physical and functional interaction between p53 and the Werner's syndrome protein. J Biol Chem 1999, 274:29463–29469